SLAC-PUB-95-7058
December 1995

BEAM-BASED ALIGNMENT OF THE FINAL FOCUS TEST BEAM *

P. Tenenbaum, D. Burke, R. Helm, J. Irwin, P. Raimondi
Stanford Linear Accelerator Center, Stanford University, Stanford, CA 94309 USA

K. Oide
National Laboratory for High-Energy Physics, KEK, Tsukuba, Japan

K. Flöttmann
Deutsches Electronen-Synchrotron, Hamburg, Germany

Beam-based alignment of quadrupole and sextupole magnets is crucial for the overall performance of linear collider final focus systems, especially for elimination of backgrounds and higher-order aberrations. At the Final Focus Test Beam (FFTB), alignment tolerances required for achieving the desired spot size are 100 microns in the horizontal and 30 microns in the vertical. Using a combination of independent magnet power supplies, high-resolution stripline beam position monitors and precision magnet movers, the FFTB can be aligned to these tolerances in about 8 hours. Description of the algorithm, presentation of alignment results, and possible improvements to the system are discussed.

1. General Concepts of Beam-Based Alignment

In order to optimize the performance of modern accelerator and collider facilities, it is necessary that the beam pass as close as possible to the center of the strong quadrupoles and sextupoles in the beamline. Consider a quadrupole with an integrated gradient G_N. A beam whose centroid passes through the quadrupole with an offset (dx, dy) from the center of the quadrupole experiences a kick given by:

$$\Delta x' = -\frac{G_N}{B\rho}dx, \qquad \Delta y' = \frac{G_N}{B\rho}dy, \tag{1}$$

where $B\rho$ is the magnetic rigidity of the beam. This kick will generate an oscillation through the quadrupoles downstream of the misaligned quad. If the amplitude of the oscillation becomes comparable in magnitude to the aperture of the beamline at some point, unacceptable backgrounds may occur due to beam "scraping". Such a kick will also introduce anomalous dispersion, which will interact with the chromaticity of downstream quads to generate higher-order chromatic aberrations. Finally, because the kick in Equation 1 is a function of quad strength, changing the optics of a beamline with misalignments will change the orbit through the beamline. Such orbit changes can prevent optical tuning from converging quickly. For all these reasons, it is necessary to reduce the RMS values of dx and dy throughout the beamline.

Now consider a sextupole with an integrated second derivative, $\int \frac{d^2B}{dr^2}dl$, given by S_N. A beam passing through such a magnet with an offset (dx, dy) from the center of the magnet receives a kick given by:

$$\Delta x' = -\frac{1}{2}\frac{S_N}{B\rho}(dx^2 - dy^2), \qquad \Delta y' = \frac{S_N}{B\rho}dxdy. \tag{2}$$

It can be shown from Equation 2 that a beam passing through a sextupole with a horizontal offset dx experiences an additional quadrupole focusing, while a beam passing through a

*Work supported by the Department of Energy, contract DE-AC03-76SF00515.

Presented at the 4th International Workshop for Accelerator Alignment,
Tsukuba, Japan, November 14-17, 1995.

sextupole with a vertical offset dy experiences an additional skew quadrupole effect. These anomalous normal and skew quadrupole aberrations will scale with sextupole strength and make the sextupole strengths difficult to tune. Once again, reducing the RMS values of dx and dy in the sextupoles of the beamline will enhance tunability.

As colliders are expected to provide greater and greater luminosities, alignment of the magnets to the beam is certain to become a more significant concern. In particular, linear colliders at very high luminosities are expected to have severe *a priori* tolerances on the RMS distance between the beam and the magnetic center for all quads and sextupoles.

Beam-based measurements – direct use of the built-in diagnostics of a beam line to measure the offsets (dx, dy) between a particular magnet and the beam – are the most straightforward method to determine the misalignments of an accelerator relative to the actual beam. In this discussion, we will limit ourselves to techniques for aligning quadrupole and sextupole magnets with the beam, although such techniques may be extended by analogy to higher-order multipole magnets.

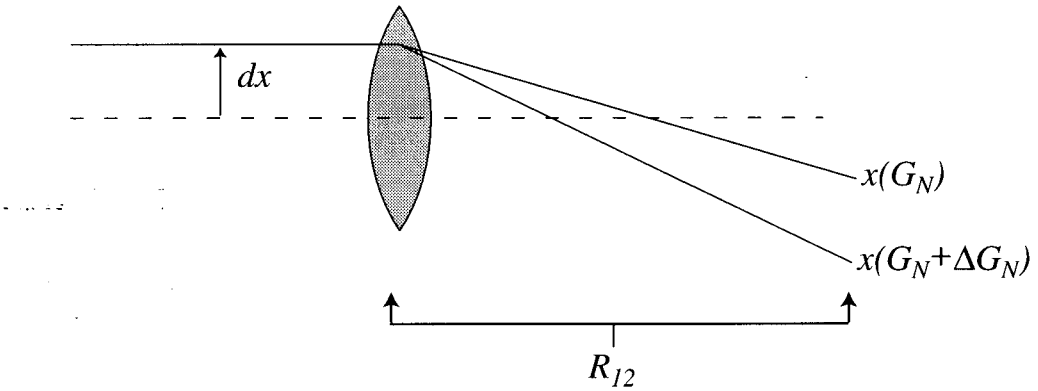

Figure 1: Quadrupole alignment via magnet shunting. Changing the quad strength changes the amplitude of the DC kick downstream.

Quadrupole Alignment: Quadrupole alignment techniques are generally extensions of the *shunt technique*: as shown in Equation 1, a beam passing off-center through a quadrupole receives a kick proportional to the quad strength and the magnitude of the offset. Consider the situation in Figure 1, in which a quadrupole with a misalignment of dx is changed in strength from G_N to $G_N + \Delta G_N$. In this case, the change in the beam position at a downstream BPM can be determined from Equation 1 and the first-order transport matrix from the quad to the BPM:

$$\Delta x = -R_{12}\frac{\Delta G_N}{B\rho}dx, \tag{3}$$

and a similar expression can be determined for the vertical plane. In this simple case the resolution of the method depends solely on the magnitude of ΔG_N, the optics from the quad to the BPM, and the BPM resolution. Once the offset dx has been determined, the quad can be moved by a distance dx to get the beam to pass through the center of the magnet.

In principle the shunt technique can be extended to a real-world system with many magnets and many BPMs used to fit the offsets $dx(j)$ and $dy(j)$. In such a case, however, there are several additional complications which must be taken into account.

Multiple Quadrupoles: Consider a situation such as that shown in Figure 2: here two quads are to be aligned to the beam, but the first quad's misalignment kicks the beam

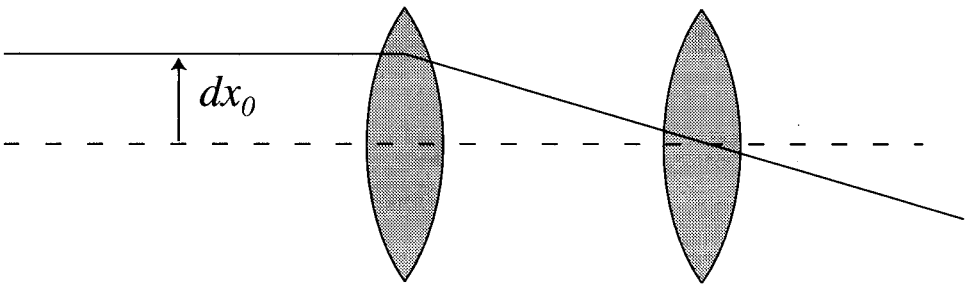

Figure 2: Beam-based alignment of two quads in sequence. The shunting procedure would indicate that the second quad is not misaligned, yet both quads need to be moved dx_0 in order to be on the line of the incoming beam.

through the center of the second quad. While shunting the first quad will reveal the misalignment dx_0, shunting the second quadrupole will show no distance between the beam centroid and the quad center at all. Clearly, the kick of the first quad must be taken into account when determining a solution which centers both quads on the trajectory of the incoming beam.

Let us define the *intrinsic misalignment* of a quadrupole, $(dx_i(j), dy_i(j))$, to be the distance between the beam centroid and the center of the jth quadrupole, as determined by the shunt technique; and define the *global misalignment*, $(dx_g(j), dy_g(j))$, to be the distance between the center of the jth quad center and the line drawn by the incoming beam, before it encounters the first quad. The relationship between the dx_i's and dx_g's is given by:

$$dx_g(j) = dx_i(j) + \sum_{k=1}^{j-1} dx_i(k) L(k \rightarrow j) \frac{G_N(k)}{B\rho}, \tag{4}$$

where $L(k \rightarrow j)$ is the longitudinal distance between the kth and jth quadrupoles. Once the dx_i values have been determined by shunting each of the quads sequentially, Equation 4 can be used to reconstruct the global misalignments; and moving each quad by $dx_g(j)$ will position all of the quads on the path of the incoming beam.

The relationship between the intrinsic misalignment resolution $\sigma_i(j)$, and the global misalignment resolution $\sigma_g(j)$, for a given quad can be derived from Equation 4, and assuming that all shunt-measurement errors are uncorrelated:

$$\sigma_g^2(j) = \sigma_i^2(j) + \sum_{k=1}^{j-1} \left[\sigma_i(k) L(k \rightarrow j) \frac{G_N(k)}{B\rho} \right]^2. \tag{5}$$

Equation 5 shows that the global alignment resolution will in general monotonically worsen from upstream quadrupoles to downstream quadrupoles. This results in the characteristic "bowing" of beam-based quadrupole alignment solutions. Such "bowing" can generally be constrained in two ways. One method constrains the beam position at the upstream and downstream ends of the region to be aligned, typically by requiring that the solution to the system maintain certain absolute BPM readings at upstream and downstream BPMs [1], [2]. In this case, the global errors will be worst near the center of the region. The other method is to constrain the beam position and angle at the entrance of the system, as was done in the FFTB. In this case the global resolution will degrade perfectly monotonically. It is important to note, however, that the RMS distance from the jth quad center to the

beam is still given by $\sigma_i(j)$. In other words, while the magnets are no longer in a straight line as measured by, for example, a laser beam, the technique outlined above will always give a solution in which the beam passes through the center of the quads to within the intrinsic resolution. Since the intrinsic alignment is the crucial one from an optical point of view, this is acceptable as long as the movements dictated by the global alignment solution do not require unacceptably large motions of the magnet.

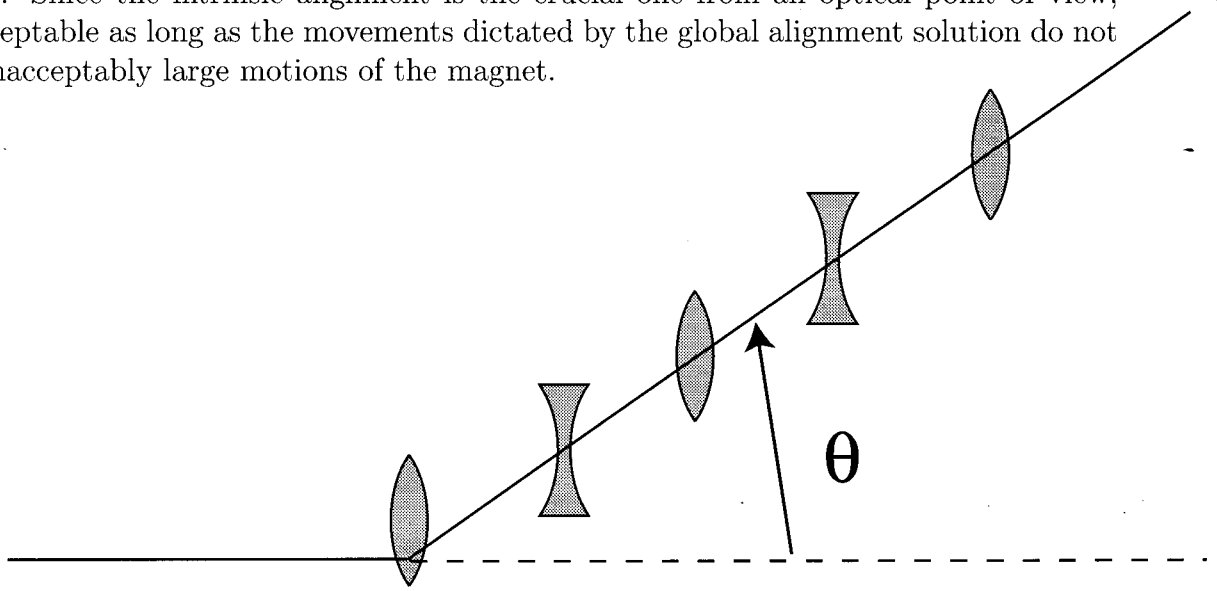

Figure 3: Alignment of a sequence of quads. In this case, the first quad in the sequence is kicking the beam onto the line of the downstream quads.

In some cases, implementing the global alignment solution in Equation 4 is not desirable from a practical point of view. Consider for example the situation depicted in Figure 3: the misalignment of the first quad results in a kick which sends the beam down the line of the remaining quadrupoles. Implementing the global solution will cause all of the quads to move onto the line of the incoming beam, resulting in monotonically-increasing movements of the magnets. For a sufficiently severe situation, the required corrections to the magnet positions exceeds that available from their installations at the downstream end. In this case the incoming beam trajectory must be adjusted to match the line of the magnets before implementing a global alignment solution. In the FFTB this was done by defining the last quadrupole in a group to be in its aligned position, and fitting the kick angle needed at the upstream end to correct the electron beam trajectory. This in turn required suitable selection of alignment segments to coincide with the availability of DC corrector magnets.

Sextupole Alignment: Techniques for the alignment of sextupoles fall broadly into two categories: those which utilize the anomalous quadrupole effect of an offset sextupole, and those which use the dipole kick given to the beam centroid. In general techniques for the use of the anomalous quadrupole field require measurements of the beam size, whereas the techniques which use the dipole field require only measurements of the beam centroid.

The quadrupole technique is used to align the CCS sextupole of the SLC Final Focus, reported elsewhere [3]: the strength of a sextupole is increased or decreased, and the beam size measured at a wire scanner is used to probe the additional quadrupole field seen by the beam. This is done by scanning a normal or skew quad at the two settings of the sextupole, and noting the value which minimizes the spot size at each setting. The strength of the normal or skew quad which minimizes the spot size is expected to be a linear function of the change in sextupole strength and of the horizontal or vertical offset, respectively, of the

beam in the sextupole. Because the SLC Final Focus sextupoles are powered in families, changing the strength of a sextupole family causes changes in the measured spot due to both sextupoles' misalignment. It is necessary to use optical symmetries of the SLC Final Focus to reconstruct symmetric and antisymmetric misalignments of the pair of magnets.

The FFTB also powers sextupole magnets in families. However, the FFTB alignment technique takes advantage of the fact that the dipole kick from the CCS sextupoles is large enough to measure with BPMs. In this technique, the beam offset in the sextupole is scanned, and the beam position is monitored downstream of the sextupole. From Equation 2, we can see that the relationship between the beam horizontal position and the offset in the sextupole is parabolic. The extremum of the parabola occurs at the point where the beam passes through the center of the sextupole. Thus scanning the beam in the horizontal and plotting downstream BPM response versus beam position reveals the horizontal center of the sextupole; while scanning the beam in the vertical and monitoring the horizontal downstream BPM response reveals the vertical center. In the case of the FFTB the sextupoles are installed on remote-controlled magnet movers capable of micron-sized motions in both vertical and horizontal, with several millimeters of total range in each direction [4]; these were used to precisely move the sextupoles across the beam path. In the absence of sextupole movers an appropriate set of corrector magnets can be used for the same purpose.

2. Application to FFTB

The Final Focus Test Beam is a prototype final focus for a future linear collider; in order to demonstrate the necessary demagnifications for such a collider the FFTB must reduce the SLAC 46.6 GeV electron beam to a focused size of 1.7 microns in the horizontal by 60 nanometers in the vertical. The optics of the FFTB have been discussed elsewhere [5], along with the *ab initio* tolerances which must be met in order to guarantee convergence of the tuning algorithm. The alignment tolerance for the quads and sextupoles is an RMS misalignment of 100 microns in the horizontal and 30 microns in the vertical. In order to ensure that these tolerances are met, an algorithm for beam-based alignment using the techniques outlined above was developed for the FFTB. This algorithm utilizes the FFTB stripline BPMs, which achieve a resolution of 1 micron at the design bunch charge [6], and the remote- controlled magnet movers for positioning the magnets. Each quadrupole is powered independently in order to simplify the shunting operation.

Quadrupole Alignment: In addition to the considerations listed above, several additional refinements of the general shunt-based quadrupole alignment procedure were needed to optimize performance.

Beam Optics: The first five quadrupoles in the FFTB are a beam matching section, with considerable flexibility to adjust the incoming beam conditions to the desired IP beam conditions. These quads were adjusted to an optics which provides a low-divergence beam at the IP (β_x^*=3 cm, β_y^*=1 cm). By reducing the IP divergence the beam size in the FFTB quads is reduced; as a result, the total range of shunting available is increased, as the quad strength changes do not have as severe an impact on the beam size downstream.

Quad Shunting: Figure 4 shows the range of quad strengths used for the FFTB standard quads, with diamonds representing the strengths in the nominal low-divergence optics. Several of the quads are shunted through 25-30% of their total range, which can cause the magnets to leave their measured hysteresis curves. This changes the optics through the FFTB in unpredictable ways; as a result, beam trajectories which are fitted from BPM

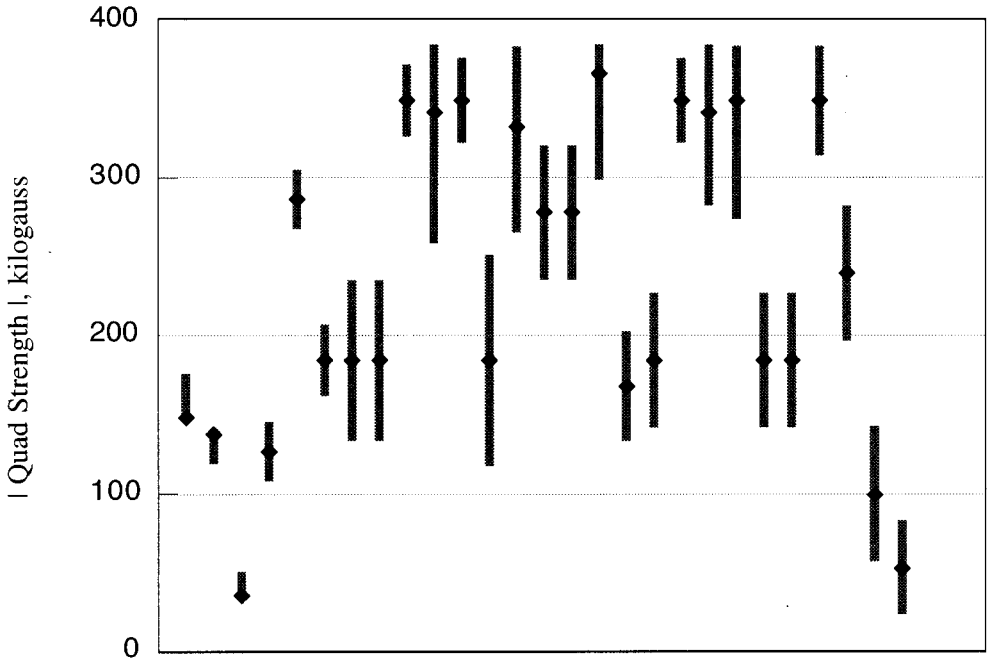

Figure 4: Shunt ranges of FFTB standard quads used for beam-based alignment. All quad strengths are shown as absolute value for ease of display. The maximum strength of the standard quad is 388 kilogauss.

data and the beamline's nominal optics will not match the actual trajectories. In order to reduce this difficulty, the quadrupole power supplies were configured to perform a "mini-standardize" procedure: when changed from a lower current to a higher current, the supply is ramped in a normal fashion, but when changed from higher current to lower current the power supply overshoots the lower set point by 5%, in order to always approach the new setpoint along a rising curve. This refinement yielded considerable improvement in overall convergence of the procedure.

BPM Data Handling: The FFTB contains 40 high-resolution BPMs with completely un-multiplexed electronics; consequently all 40 BPMs can be read out on a single pulse. For alignment of a single segment consisting of 3 to 6 quads, a total of 150 beam pulses is acquired on all BPMs. Such a large dataset may well contain data points contaminated by unacceptable noise, which must be eliminated before fitting the misalignments of the quads. Furthermore, the pulse-to-pulse jitter at some BPMs is as large as 40 microns in RMS, and this jitter must be corrected in order to achieve the maximal performance from the high-resolution BPMs. A set of 6 quadrupoles with horizontal and vertical misalignments contains 12 variables to be fit, while a set of 150 pulses with incoming (x, x', y, y', δ) to be fit contains 750 variables. Finally, because of incoming jitter, it is necessary to be certain that the trajectory of the inital pulse, to which the quads will be aligned, is not extremely different from the average of the linac beam pulses.

The initial orbit to which the beams will be aligned is determined by averaging 100 pulses to derive a representative reference orbit. This orbit is then compared to incoming orbits to ensure that it is not systematically different from the incoming beam. This orbit is subtracted from all the subsequent orbits, leaving only the differences from the reference

at each BPM. The incoming trajectory vector for each pulse, (x, x', y, y', δ), is determined by using BPMs in areas upstream and downstream of the shunted quads, in areas where the transport properties are constant. This computation is done by matrix inversion, yielding an incoming ray and a full error matrix for the incoming trajectory. Because the main fit will ultimately use ray- tracking to determine the misalignments, it is vital that the error contribution from the determination of the incoming beam trajectory be added to the instrumental error contribution from the BPM resolution. This is accomplished by projecting the error matrix for the incoming beam onto each BPM and adding the (11) or (33) component of the projected error matrix in quadrature with the instrumental resolution. Finally, the transport properties downstream of the last shunted quadrupole are also constant; therefore the BPM readings through this area should fit to some initial trajectory at the downstream face of the last shunted quadrupole. Fitting the trajectory at the exit of the last shunted quad with the data from downstream BPMs aids in identifying noise-dominated data: such data will not lie upon the fitted ray. Thus the bad data is identified and eliminated before submitting the BPM data to the main fitting algorithm.

Main Fitting Algorithm: The main fitting algorithm uses first-order ray tracking and MINUIT χ^2 minimization to determine the offsets of the quadrupoles. The returned offsets and alignment resolutions are for the global alignment, i.e., the alignment of all the quads to the common incoming line.

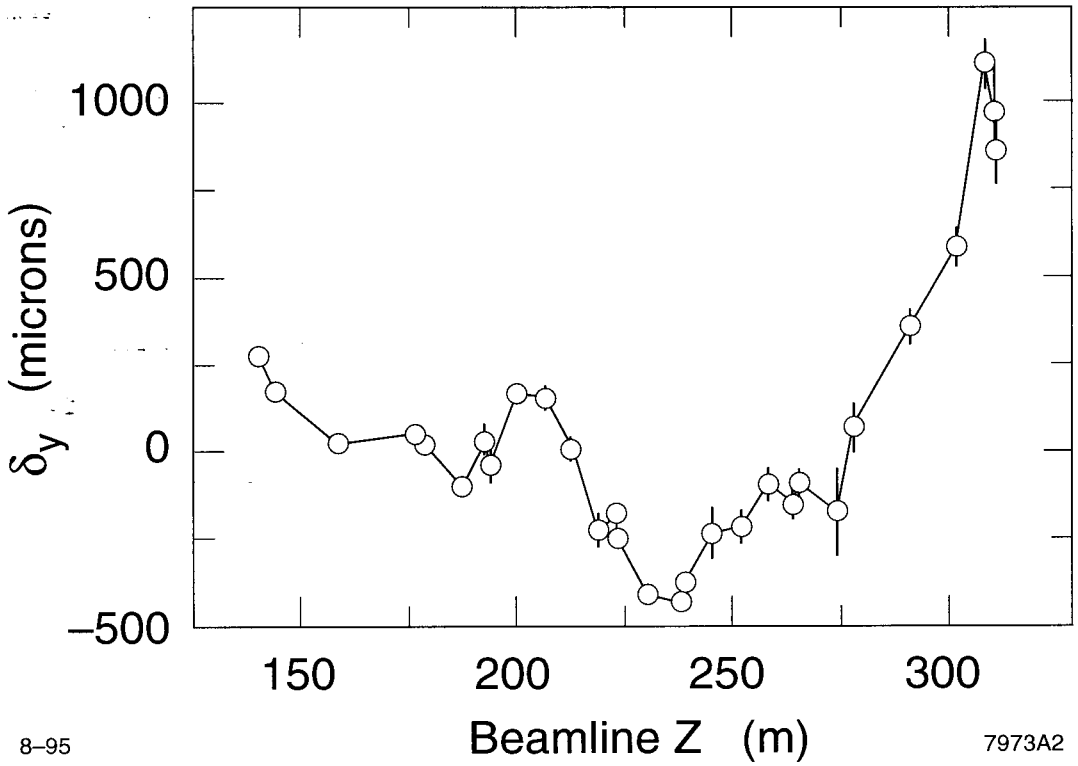

Figure 5: Measured vertical locations of FFTB quads relative to the incoming beam, May 1994. Note that the large excursions exceeded the range of the remote-control movers, and DC correctors were required.

Results of Quadrupole Alignment: Figure 5 shows the vertical positions of the quadrupole centers with respect to the incoming beam, as determined in May of 1994. Because of the large displacements it was not possible to move all the magnets into their

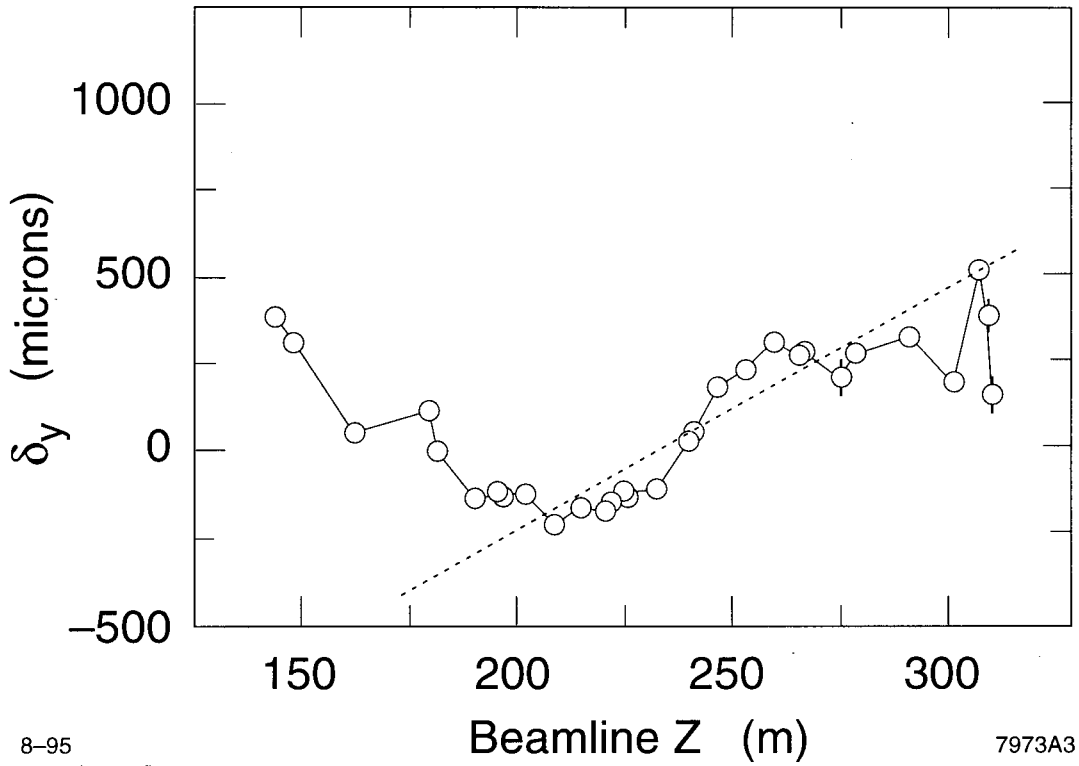

Figure 6: Measured vertical positions of FFTB quads relative to the incoming beam, September 1994. During the period between May and September 1994 the magnet alignment was mechanically corrected, and the FFTB was able to operate in September 1994 with no vertical correctors. The dashed line shows the best line through the region surveyed.

aligned positions with their remote- controlled movers; instead, several DC correctors were used to steer the beam through the line.

After the experience of May 1994, the FFTB was surveyed by the mechanical alignment specialists at SLAC, and qualitatively-similar alignment features to those in Figure 5 were seen. These were corrected mechanically, and the beam-based alignment repeated in September of 1994. Figure 6 shows the measured magnet positions in September 1994. The dotted line represents the best line through the quads surveyed mechanically; the RMS deviation from the line is approximately 50 microns, representing the alignment resolution available through mechanical survey. In this case the FFTB was able to operate with no vertical or horizontal correctors upstream of the IP, save for two which adjust the position and angle in each plane to match the mechanical line.

Intrinsic resolutions returned by the MINUIT fit revealed worst-case resolutions of 30 microns for two magnets, with the majority of magnets aligned to within 10 microns in each plane. The worst-case global alignment resolution was found to be 350 microns at the downstream end of the beamline, which is handily within the range of remote- controlled movers. It was also observed that the beam-based alignment reduced a measured vertical dispersion by a factor of 3, and that background tuning converged more quickly and more completely after complete beam-based alignment.

Sextupole Alignment: The CCS sextupoles were aligned in the manner described above, in which each sextupole in turn was moved across the beam and its motions corre-

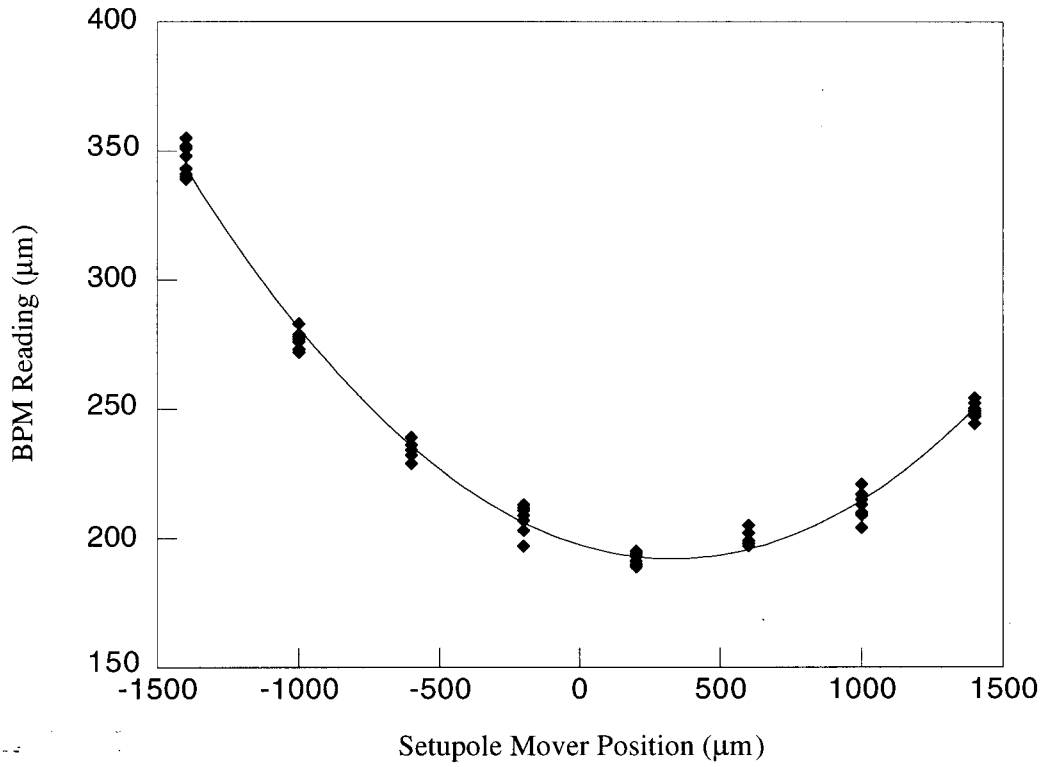

Figure 7: Downstream BPM horizontal position as a function of sextupole vertical mover position. The minimum of the parabola is the mover position which causes the electron beam to pass through the vertical center of the sextupole.

lated with horizontal positions downstream. No jitter correction was performed, and some care was exercised to determine for each sextupole a BPM which optimized the signal-to-noise performance of the algorithm. Figure 7 shows the downstream BPM signal as a function of vertical mover position for one sextupole, with a clearly- defined minimum corresponding to the vertical center position of the magnet. The resolution of the procedure was 25 microns or better for each sextupole in each plane, with some improvement possible if jitter correction was included in the fit.

3. Conclusions and Possible Improvements

The FFTB beam-based alignment algorithm allows the beamline to be aligned to within its tuning tolerances in approximately 8 hours. All alignment is completed with relatively large beam sizes at the IP, and can therefore be performed before any IP tuning is attempted. Of the 8 hours, 1 hour is required to align the 4 CCS sextupoles, with the 7 hours of quadrupole alignment being divided in a 70:30 ratio between stepping quadrupole power supplies and computation. Acquisition of BPM data is a negligible contributor to the total time.

The most significant improvement to the system would be reduction in either the shunting or computing time requirements. Computing time could be reduced through implementation of a matrix-inversion solution to the quadrupole offset problem, rather than MINUIT, or of

course through use of a faster computer. The quad shunting time is determined by the current ramp rates used by the power supplies; these in turn have been adjusted to match the ramp rates used when the magnetic fields were measured. Some further optimization of the current ramping rate is conceivably possible.

The cuts applied to the downstream data are computationally efficient but are not the best possible for eliminating bad data. Once a track has been fit, any BPM which has a χ^2 contribution greater than 64 per data point is eliminated; a second fit is performed, and any BPM with a χ^2 contribution greater than 16 is eliminated; finally, a third fit is performed and individual data points with χ^2 contributions greater than 16 are eliminated. The cutting algorithm can be "fooled", especially in cases in which a single BPM at a critical point in the optics can alter the fit significantly; in this case, it is not unusual to find that all BPMs have large χ^2 contributions and are eliminated. A more robust algorithm would fit a track to each of the 150 BPM pulses; then, for each pulse with a χ^2/ν greater than some cutoff, the fit is repeated n times, where n is the number of BPMs used in the fit; each of the n fits would be performed without one of the BPMs. The data point which caused the largest increase in χ^2/ν could thus be unambiguously identified and eliminated. This scheme is, however, more computationally intense.

Finally, the advantage of jitter subtraction in the sextupole alignment algorithm has been noted above.

Acknowledgements

The authors wish to thank Lee Ann Yasukawa for writing the Quad Alignment interface software in the SLAC Control System.

References

[1] P. Emma *et al.* "Beam-Based Alignment of Sector 1 of the SLC Linac." Proceedings of the 1992 European Particle Accelerator Conference, 1625 (1992).

[2] C. Adolphsen *et al.* "Beam-Based Alignment Technique for the SLC Linac." Proceedings of the 1989 IEEE Particle Accelerator Conference, 977 (1989).

[3] P. Emma *et al.* "Beam-Based Alignment of the SLC Final Focus Sextupoles." Proceedings of the 1993 IEEE Particle Accelerator Conference, 116 (1993).

[4] G. Bowden *et al.* "Precision Magnet Movers for the Final Focus Test Beam." To be published in Nuclear Instruments and Methods A.

[5] K. Oide. "Design of Optics for the Final Focus Test Beam." Proceedings of the 1989 IEEE Particle Accelerator Conference, 1319 (1989).

[6] H. Hayano *et al.* "High-Resolution BPM for FFTB." Nuclear Instruments and Methods **A320** 47 (1992).